Effect of roof diaphragm on masonry structures under dynamic loading

Navaratnarajah Sathiparan[*]

Department of Civil and Environmental Engineering, Faculty of Engineering, University of Ruhuna, SriLanka

Abstract. The structural collapse of masonry structure under dynamic loading displays many possible failure mechanisms often related to interaction between structural components. Roof collapse is one of the major damage mechanisms observed in masonry structures during an earthquake. Better connection between the roof diaphragm and walls may be preventing roof collapse, but it can affect other failure mechanisms. In spite of this fact, less attention has been paid to the influence of the roof diaphragm effect on masonry structures and little research has been implemented in this field. In the present study, the roof diaphragm effect on the unreinforced masonry structure under dynamic loading has been experimentally investigated. Three one-quarter scale one-story adobe masonry house models with different roof conditions have been tested by subjecting them to sinusoid loading on a shaking table simulator. Phenomena such as failure pattern, dynamic performance of masonry structure were examined.

Keywords: masonry; roof diaphragm; shaking table test; shear resistance; drift

1. Introduction

Past earthquakes have emphasized the vulnerability of the masonry structures, mostly due to the lack of effective connection between structural components. Major types of damage patterns observed during earthquakes in this type of building;
- In-plane failures
- Out-of-plane failures
- Failure due to lack of corner connections
- Diaphragm related failures
- Material disgregation (in poor earthen masonry)
- Delamination (in multi-leaf walls with poor mortar)

Unreinforced masonry structures are in fact characterized by weak connections between the different structural elements and tend to exhibit collapses. Horizontal inertia force development at the roof transfers to the walls acting either in the weak or in the strong direction. If all the walls are not tied together like a box, the walls loaded in their weak direction tend to out-of-plane failure. To ensure good seismic performance of masonry structures, all walls must be joined properly to the

---

∗Corresponding author, Ph.D., E-mail: nsakthiparan@yahoo.com

adjacent walls. An addition to the connection between orthogonal wall, the flexibility of the roof/floor diagrams and their connection to the masonry walls are main factors to take into account for capability to distribute the seismic loads (Lourenço *et al*. 2011). The seismic response of the masonry structures to past earthquake showed that the adequate anchorage of unreinforced masonry walls to the floor/roof diaphragm can enhance the global seismic performance in a significant way. When a masonry wall not properly connected to the roof or floor, it can easily become unstable and collapse on out-of-plane (Araújo *et al*. 2014). Simsir *et al*. (2004) reported that diaphragm flexibility, increased the out-of-plane displacement response and significantly amplified the diaphragm mid-span displacement and acceleration responses with respect to those of the in-plane walls. Therefore, the stiffness and connection of roofs and floors are important for earthquake resistance (ICBO 1997).

Consider the one story box shape masonry house shown in Fig. 1, there are three possible types of roof diaphragm conditions, mainly house without roof, roof connected to two parallel walls of the house and roof connected to all four walls of the house. When considering the house without a roof, wall parallel to ground motion direction act as shear wall and it offer resistance against the collapse of adjacent walls. If the connection between these two adjacent walls is not lost due to corner failure, the building will tend to act as a box and its resistance to horizontal loads will be adequate. But most unreinforced masonry house have weak vertical joints between adjacent walls due to the construction procedure involving toothed joint that is generally not properly filled with mortar. Consequently the corners fail and lead to collapse of the walls. In case of roof connected to two walls, roof transfer its inertia force at the top of walls parallel to ground motion direction, causing shearing and bending action to them. If these walls have enough shear strength, it can withstand the force induced by a roof or shaking motion. But that wall subjected to ground motion perpendicular to its plane, it can collapse very easily because those walls have little out-of-plane bending resistance in the plane perpendicular to it. If roof connected all four walls, it can act as a horizontal diaphragm; its inertia will be distributed to the four walls in proportion to their stiffness. By means of the roof connection provisions, the integrity of an existing building can be enhanced.

The connection between walls and floor diaphragms are greatly affecting the seismic response of masonry structures (Rota *et al*. 2011). The effect of floor/roof in masonry structures has been studied by a few researchers, either evaluating the behavior of the single wall or global behavior of the building. Dynamic tests on one-fourth scale, two-story, stone masonry buildings with different types of floor systems were discussed by Tomazevic *et al*. (1992). Results indicated that the type
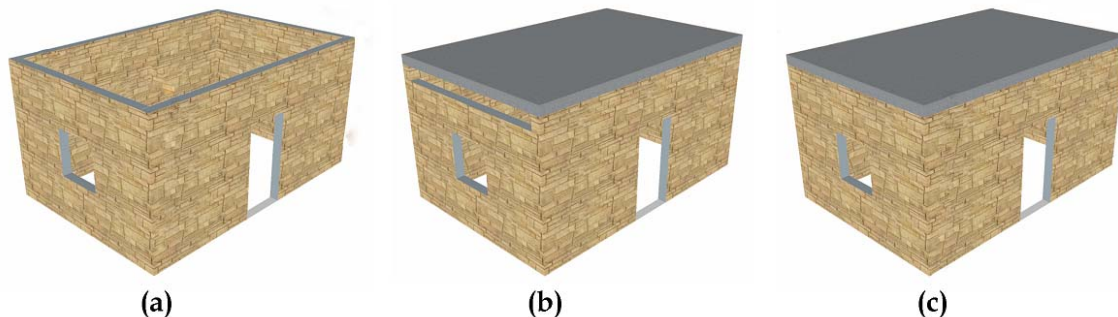

Fig. 1 Different wall enclosure condition at roof level: (a) house without a roof (b) roof connected to two walls of the house and (c) roof connected to all four walls of the house

of floor system was less important than how well the floor system was connected to the walls and how well the walls were tied together.

An experimental program was recently carried out at the European Centre for Training and Research in Earthquake Engineering (EUCENTRE, Italy) aimed at studying the seismic response of double leaf stone masonry buildings with timber floor and roof in which different levels of strengthening interventions improving diaphragm stiffness and diaphragm-to-wall connections were simulated. The interventions applied were meant, at different levels, to improve the wall-to-diaphragm connections and to increase the in-plane stiffness of diaphragms and permitted to ensure a global type of response and to prevent the occurrence of out-of-plane local failure mechanisms (Magenes *et al*. 2013, Senaldi *et al*. 2013). Results show that the improvement of the wall to floor diaphragm connections proved to be very effective, increasing significantly the seismic capacity of the structure (Magenes *et al*. 2014).

The main reason that motivated the present research was the scarce experimental information on roof diagram effect on masonry structure. Therefore, this study was aimed at understanding of the roof diagram effect by testing masonry house models to determine the dynamic behaviour of the models. One-quarter scale one story adobe masonry house model was chosen for this study; and shaking table tests on models with three roof conditions were performed.

2. Description of specimen and experimental procedure

2.1 Description of specimen

A comprehensive testing program on the dynamic performance of the adobe masonry house has been undertaken. As shown in the Fig. 2, the one-quarter scale single story house model was a box with dimensions 933 mm×933 mm×720 mm with wall thickness of 50 mm. A single door was 243 mm×485 mm and window on the opposite wall was 325 mm×245 mm. The lintel over the door and window were made of wooden with dimensions $390 \times 50 \times 35$ mm^3 and $470 \times 50 \times 35$ mm^3, respectively. The overall dimensions of the specimen were limited by the size and capacity of the shaking table. Weight of the house model without roof, and weight of roof were 255 kg and 15 kg, respectively.

The shaking table system at Institute of Industrial Science, The University of Tokyo is capable of controlling six degrees of freedom. The steel platform measured 1.5 m×1.5 m in plan, and could carry a maximum payload of 2,000 kg. It was capable of operating at frequencies ranging from 0.1 to 50 Hz. The maximum acceleration input, under zero payloads, was ±2.0 g in the longitudinal direction and the maximum displacement was ±100 mm (Sathiparan and Meguro 2012). In this experiment, the controlling shaking table system was limited to one direction shaking for simplicity of motion.

Three models of simple buildings were constructed in this experimental program. In three models, first model represented a box-type one story building without a roof. Although it is preferred to have the roof in model 1 without connecting to walls, emphasize that the prototype has usually small roof. Major problem in using roof in the model 1 is sliding of the roof during shaking and may introduce local failure. The second model represented a box-type one story building with timber roof and the roof is connected to north and south walls. The third model was built similar to second model except the roof is connected to all four walls.
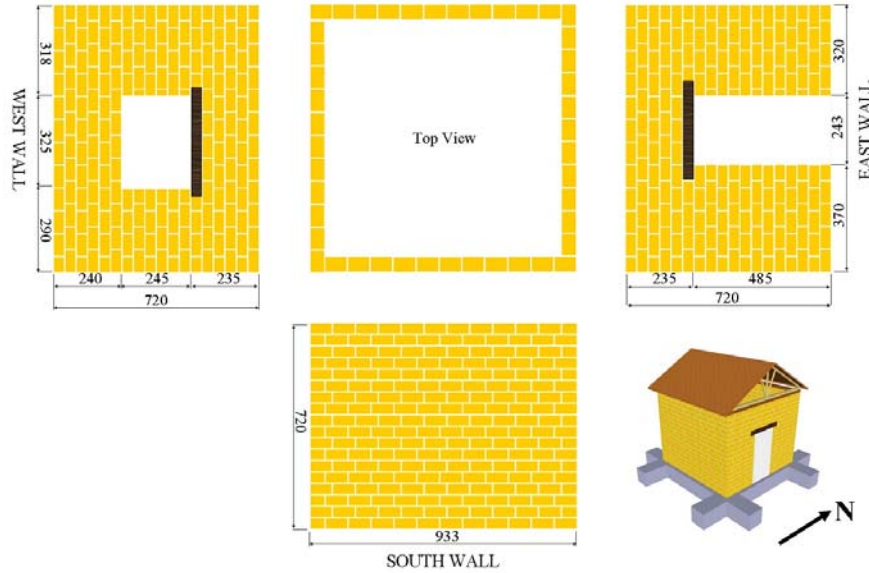
Fig. 2 House model for shake table tests (dimensions in mm)

2.2 Construction of the house models

A reinforced concrete pad was designed and constructed to provide a foundation for the house models. The house models were consisted of 18 rows of 44 bricks in each layer, except openings. Construction of the model took place over two days, with the first 11 rows built on the first day and remaining rows constructed in the following day. The geometry, construction materials and mixture proportion, construction process and technique and other conditions that could have affected the strength of the house models were kept identical. For the construction, the adobe unit having the size of 75 mm×50 mm×35 mm and mortar material with cement: sand: lime in 1:2.8:8.5 weight proportion was used.

2.3 Masonry Properties

During construction of the models, material tests were conducted to obtain the mechanical properties of the masonry. Masonry prisms were tested to evaluate the masonry's strength in compression, shear and tensile bond. The layout of specimens used for the direct compression, direct shear, and bond tests is shown in Fig. 3 (Sathiparan *et al*. 2005). The axial compression tests and shear tests were performed under displacement control, according to BS EN 1052-1 and BS EN 1052-3 (BSI, 1999; BSI 2002). The dimension of the specimens used for the diagonal shear test were 275×275×50 mm^3 and consisted of 7 bricks rows of 3.5 bricks each with the mortar joint thickness was 5mm. ASTM E519/ E519M-10 standard (ASTM 2010) guidelines were used to investigate the in-plane diagonal shear strength of masonry. The experimentally measured diagonal force, *P* was transformed into diagonal shear strength (τ) as
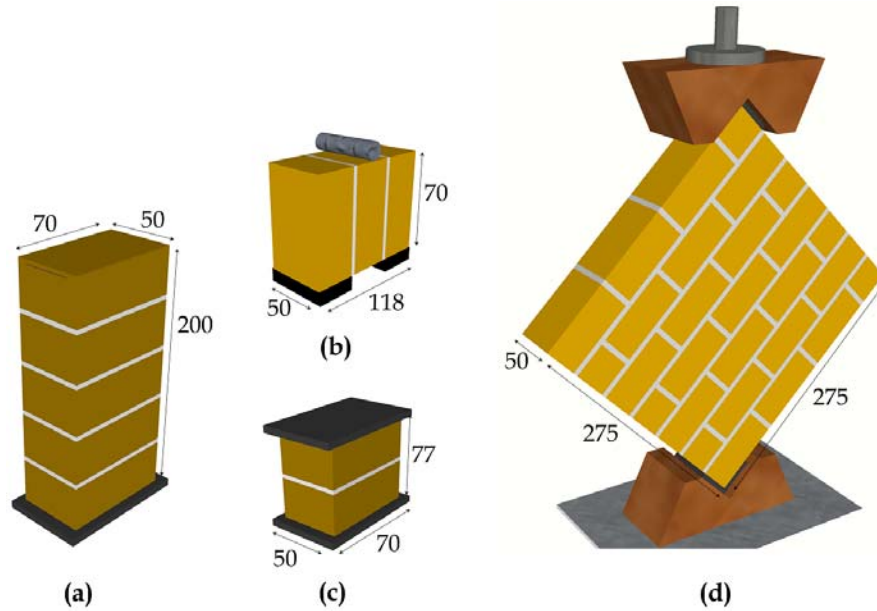
$$\tau = \frac{0.707 P}{0.5t(L + H)} \tag{1}$$

Fig. 3 Dimension of the specimen used for material testing (in mm) (a) compression, (b) shear, (c) tensile bond, and (d) diagonal shear

Table 1 Specimen mechanical properties

	House model		
	1	2	3
Compression strength (MPa)	4.40	4.33	4.28
Shear strength (kPa)	6.4	6.5	5.7
Bond strength (kPa)	4.5	5.2	4.6
Diagonal shear strength (kPa)	42	46	41

where t is specimen thickness, L is specimen length and H is specimen height. The resulting compressive, tensile and shear strength of masonry were listed in Table 1.

2.4 Roof diaphragm

For these models, wooden truss roof was adopted, above which, two inclined plywood sheet with a dimension of 1033 mm×600 mm and 10 mm thick were attached. Roof sheathing consisted of 10 mm thick plywood nailed to the sloping edges of the trusses using 25 mm long nail at 150 mm intervals. The roof diaphragm was connected to the top of the masonry walls using 10 mm diameter bolt at 160 mm intervals as shown in the Fig. 4. In between masonry wall and roof rafter, 5 mm cement-sand mortar was provided.

2.5 Test procedure

Simple and easy-to-use harmonic motions with frequencies ranging from 2 to 35 Hz and

Fig. 4 Wall connection detail of roof to wall

Table 2 Shaking table test run sequence (Sathiparan *et al*. 2012)

| | | Frequency (Hz) | | | | | | | |
		35	30	25	20	15	10	5	2
	sweep				01, 02				
	0.05 g	03	04	05	06	07	08	09	10
	0.1 g	11	12	13	14	15	16	17	18
Amplitude	0.2 g	19	20	21	22	23	24	25	
	0.4 g	26	29	32	35	38	41	44	
	0.6 g	27	30	33	36	39	42	45	
	0.8 g	28	31	34	37	40	43		

amplitudes ranging from 0.05 to 0.8 g were applied to the specimens to obtain the dynamic response of house models. The run numbers are shown in Table 2. Shaking table motions were applied sequentially, starting with low intensities and increasing until collapse was observed. In this test sequence, the test structures were damaged gradually, and were already in a weakened condition when subjected to the high intensity motions. Therefore, it was possible observed the progressive damage of the house models.

The time-history response of the models was measured by accelerators and laser displacement measuring instruments. As shown in the Fig. 5, the displacements of the diaphragm were measured at the corner, quarter and middle points. Base displacement was measured to get the relative deformation of the diaphragm. Another laser measurement was recorded the facade wall deformation at the centre. In the house model eleven accelerometers, seven on top of the walls, two in the base and two on the roof were installed. The measured data were recorded continuously throughout the tests. The sampling rate was 500 Hz.
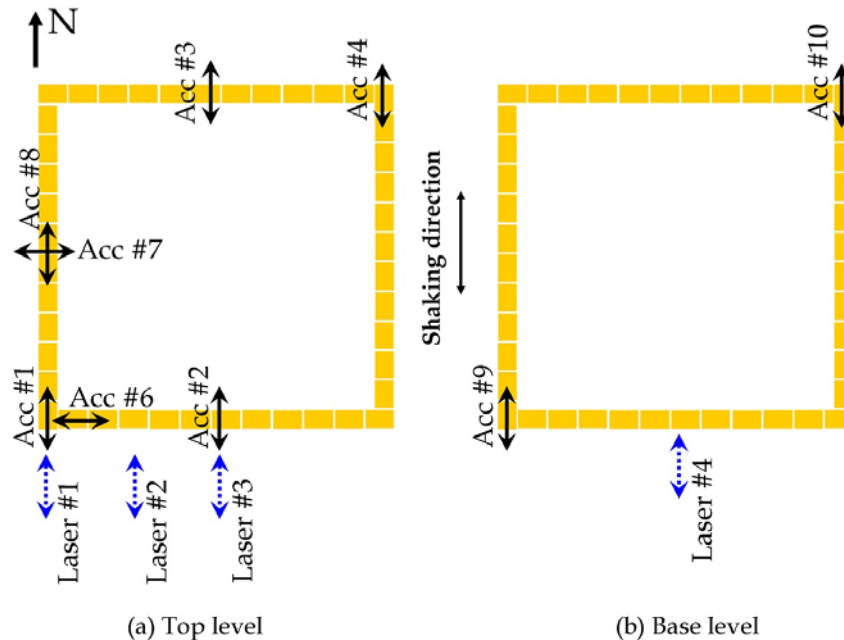
Fig. 5 Model house instrumentation position

Table 3 Difference and the consequences of scale model and prototype

Constraints	Test model	Prototype	Consequences for the test
Scale of house	Plan area: 0.93 m×0.93 m height: 0.72 m	Plan area: 3.6 m×3.6 m height: 2.5~3.0 m	A full-scale test made it possible to obtain data similar to real structures. However, it required large testing facilities and a significant amount of research funding. The wall ratio is 1/4 due to the ratio of area to wall thickness. Because the subject house was a single story, there were no discrepancies in the test results.
Adobe unit	Japanese made adobe unit	Sun burned adobe made of clay	Adobe from Japan is most desirable for shape and accuracy, and the strength of the product. However, there are no consequences to the strength of the wall, specifically because it depends on the strength of the bond.
Joint mortar	Cement: sand: lime in 1:2.8:8.5 in weight	Mud mortar	Very weak mortar mix was used in order replicate low strength mortar.
Input load	Sinusoid loading with increasing intensities	Seismic loading	Test structures experienced gradual damage, and were already in a weakened condition when subjected to high intensity motions. However, with this test procedure, it was possible to observe the progressive damage to the model houses.

2.6 Test constraints

Shaking table tests were intended to reproduce the behaviour of an actual house in developing countries. However, there were some difference between the houses in the test-model and the prototype model. Those points of differences and the consequences are shown in Table 3.

3. Experimental results

In all three specimens, due to shrinkage, some minor cracks were observed prior to testing. These cracks appeared primarily above the openings, in the horizontal direction. With the exception of those cracks, no major cracking was observed up to run 24.

3.1 House model 1

Fig. 6(a) shows the crack pattern for model 1 after run 25. The cracks appeared primarily above the lintel of the window opening. With the exception of those cracks, no major cracking was observed. At run 34, many cracks were observed at the corner of the window and door opening.
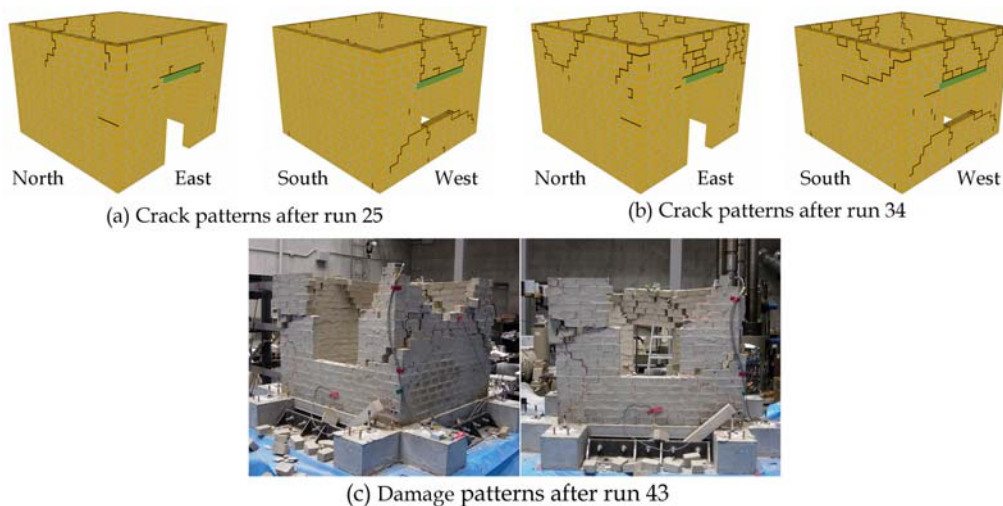

(a) Crack patterns after run 25   (b) Crack patterns after run 34

(c) Damage patterns after run 43

Fig. 6 Crack patterns and damage pattern observed in model 1

(a) Crack patterns after run 25   (b) Crack patterns after run 34

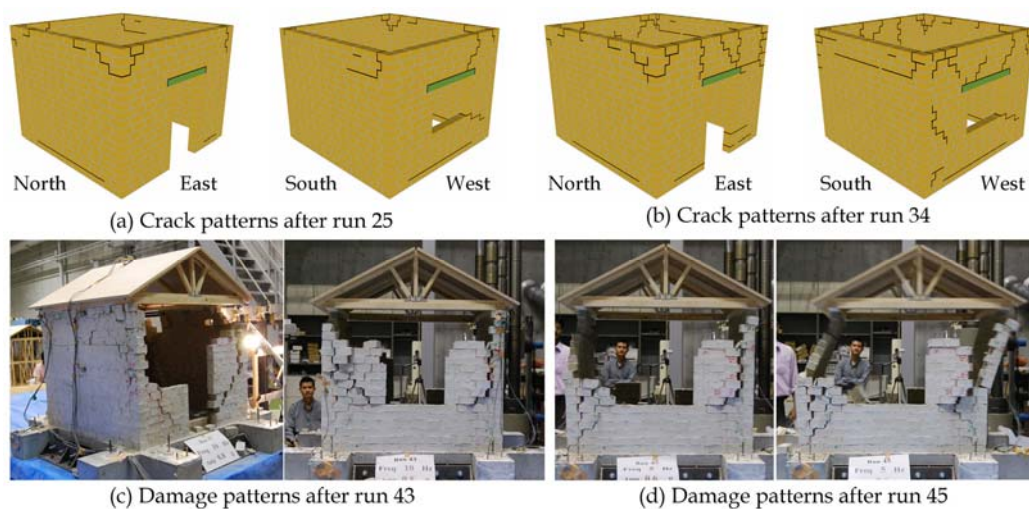(c) Damage patterns after run 43   (d) Damage patterns after run 45

Fig. 7 Crack patterns and damage pattern observed in model 2

These cracks propagated towards the top layer of the wall (Fig. 6(b)).

At run 40, the extensive cracks appeared in the west and east walls, parallel to the shaking direction, due to in-plane actions. These were followed by cracks in the north and south walls, due to out-of-plane actions. In addition to that, partial separation of walls at the corners was observed. Although, cracks widened with each successive run after run 40, run 43 more critical. During this run, a portion of the wall above the window opening was separated totally from the model (Fig. 6(c)). Also, some part of the south side wall separated and collapsed from the model. On the next run, these cracks become wider and connections between adjacent walls become weaker. As a result, each wall was becoming an independent structure, which is the worst-case scenario where walls supported only at the bottom. Therefore, due to walls subjected to out-of-plane load, they were collapsed in the direction of shaking.

3.2 House model 2

After run 25, the model 2 damage level was less compared to the model 1. Crack mainly appeared close to the openings and it reached the top layer of the wall. Also, some cracks were observed at top corner of the adjacent walls (Fig. 7(a)).

At run 34, more cracks observed at the top part of the east wall, where the door was located. Also, one long horizontal crack observed at the top part of the north wall (Fig. 7(b)). At run 40, there were many cracks observed in the north and south walls. Existing cracks widened and connections between adjacent walls become weaker. The top portion of the wall above the door lintel separated totally from the model. After two more runs, left top corner portion of the west wall and right top corner portions of the east wall were separated totally from the model.

At the end of run 43, the entire top portion of the wall above the door and window opening separated totally from the model (Fig. 7(c)). At this point, the roof was supported by only two walls, which were in the direction of shaking. Therefore, during the next run, due to out-of-plane load; the walls burst outward in the direction of shaking. This finally led to the collapse of the structure (Fig. 7(d)).

3.3 House model 3

Fig. 8(a) shows the crack pattern for model 3 after run 25. Up to this point, the cracks look lesser and seem no damage on the east wall compare with other two models. But in general, the crack appearance closer to opening was similar. At run 34, inclined cracks appeared that began at the corner of the opening on the west wall, where the window was located, and reached the top and bottom of the model. In the east wall, where the door was located, the inclined cracks were accompanied by horizontal cracks that reached the north and south walls. In addition to that, horizontal flexural crack on the top layer of the north and south walls was observed (Fig. 8(b)). Although the cracks widened with each successive run after run 39, run 43 was critical. Fig. 8(c) shows the house model after run 43. There were many cracks observed in the walls in the direction of shaking. These became wider at higher excitations and as the connection between adjacent walls become weaker. At the end of run 44, the portion of the wall above the door lintel separated totally from the model. During run 45, the entire top portion of the wall above the door and window lintel separated from the house model and collapsed (Fig. 8(d)). At this point, the roof was supported by only two walls. Due to these walls subjected to out-of-plane load, the walls burst outwards in the direction of shaking. This finally led to the collapse of the structure.
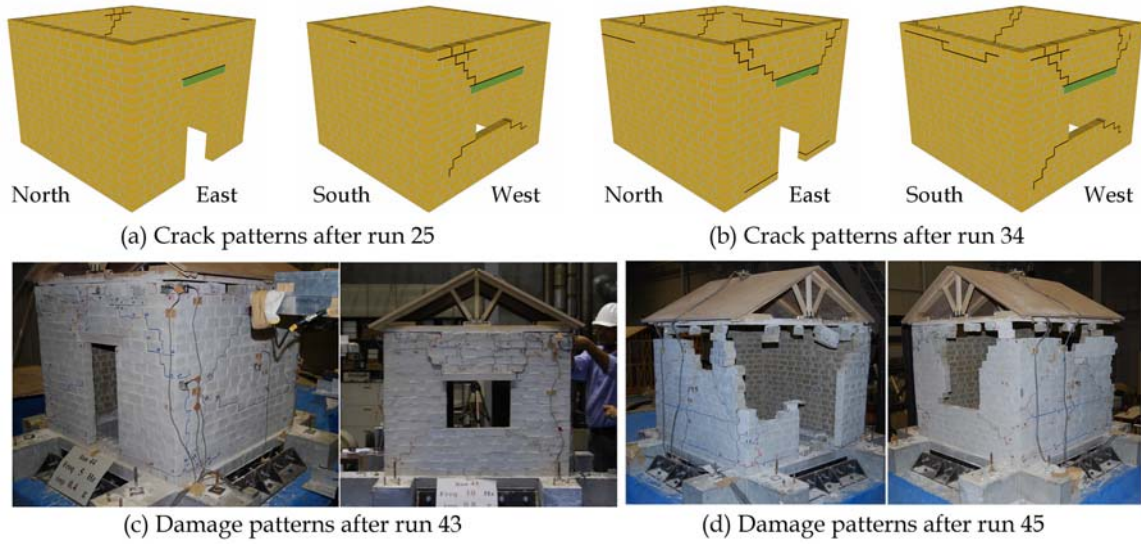
(a) Crack patterns after run 25   (b) Crack patterns after run 34

(c) Damage patterns after run 43   (d) Damage patterns after run 45

Fig. 8 Crack patterns and damage pattern observed in model 3

3.4 Failure comparison

In case of model 1, out-of-plane force during shaking acted on north and south walls tend to overturn it. The out-of-plane seismic strength of the wall is depending on its self-weight, the tensile strength of mortar, and the connection to transverse walls. Due to free end at the top, the seismic resistance against out-of-plane force was obviously very small. These walls initially collapsed by overturning under the shaking motion. Consequently the vertical joints between wall connections become weaker and the corners failure leads to collapse of the house model. But in case of the other two models, failure initiated in east and west walls due to in-plane force. Due to in-plane failure, the roof supported only by north and south walls; they were bursted outwards during shaking. This finally led to the collapse of the model 2 and 3.

4. Analysis of results

4.1 Vibration response

For each test run, the intensity of the table motion was evaluated using the cumulative absolute velocity of the shaking table input motion. These are possible measures of the potential damage and cumulative effects of continued ground motion. The cumulative absolute velocity (CAV) is calculated by Eq. (2) (Benjamin 1988)

$$CAV = \int_0^{t_{max}} |a(t)| dt \qquad (2)$$

where $|a(t)|$ is the absolute value of the acceleration time series and t_{max} is the total duration of the shaking table input.
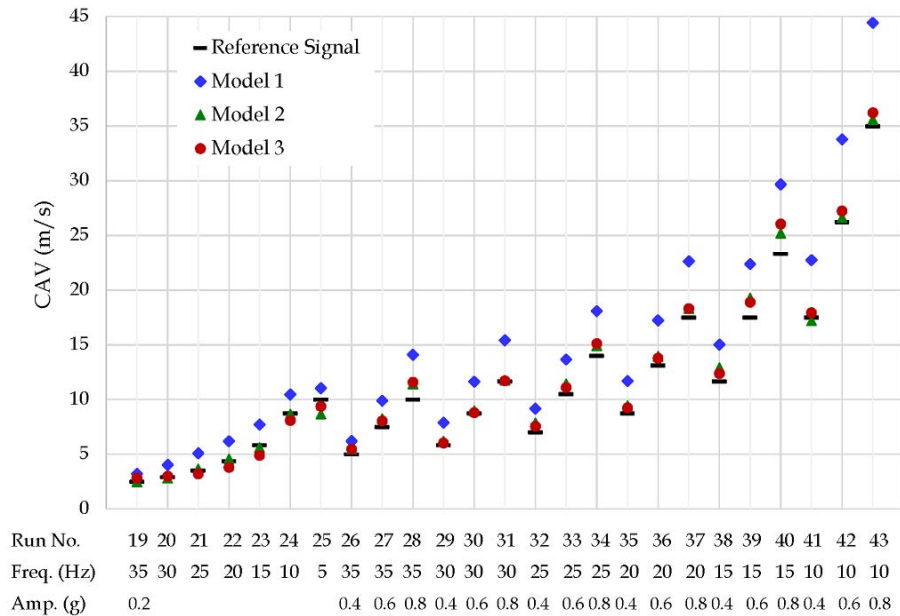
Fig. 9 Cumulative Absolute Velocity of the models

The acceleration imposed by the shaking table did not show a perfect agreement with the reference input motion because of the dynamic interaction between the shaking table and the structure to be tested. The discrepancy between the reference acceleration and the actual feedback from the shaking table is reflected by the differences between the reference and house model CAV measured, as reported in Fig. 9. The model 1 was subjected to a much higher intensity of shaking in comparison to reference input motion, with values that are almost 30% larger than expected ones in terms of CAV. But in case of model 2 and 3, even for higher intensity input motion, only around 8 % larger than expected one. It indicates these two models; the motion of the test structures followed the shaking table motion very closely, with distortions generally proportional to, and in phase with the base acceleration.

4.2 Deformation compression

Lateral story drift is another dimensionless parameter which can be used to compare the models, being the lateral displacement at the top corner of the wall divided by the height of the wall. Same way diaphragm drift can define as mid wall displacement at roof level divided by the length of the wall (Fig. 10). Using the recorded displacement values of laser displacement measuring instruments (L1, L3 and L4) the displacement profiles of the walls was constructed.

Figs. 11, 12 shows the story drift and diaphragm drift correspond to peak base velocity of shaking table input motion. In house models 2 and 3, behaved noticeably better than model 1 during all test runs. Compare with model 1, lateral story drift 24% and 32% less for model 2 and 3, respectively. In case diaphragm drift, models 2 and 3 drift 65 % and 72% less than that of model 1, respectively. These results show that; better roof diaphragm integrity controls the deformation of the wall during shaking.
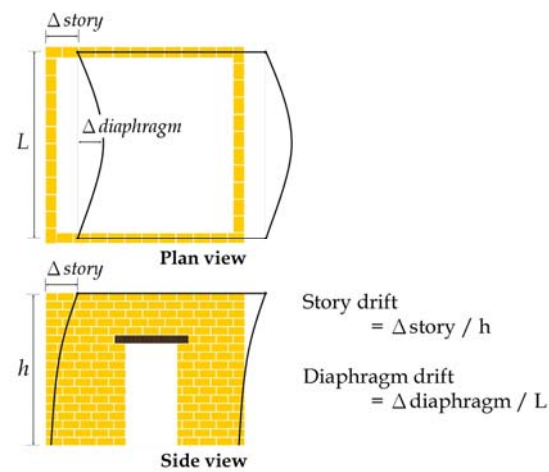
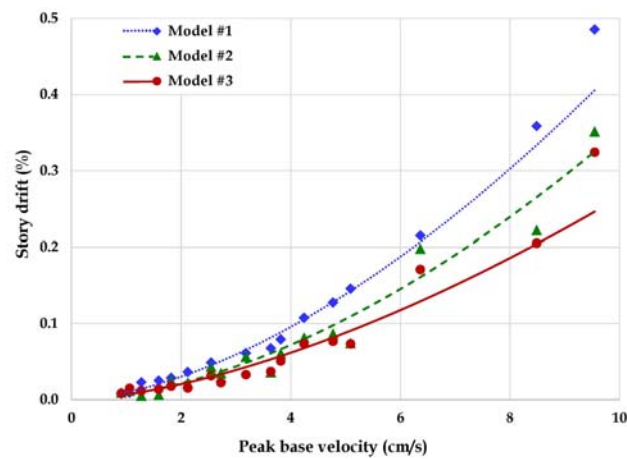Fig. 10 Define the story drift and diaphragm drift

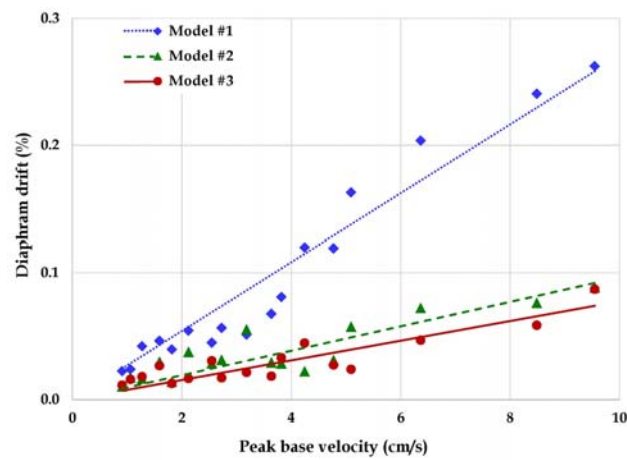Fig. 11 Story drifts variation with peak base velocity

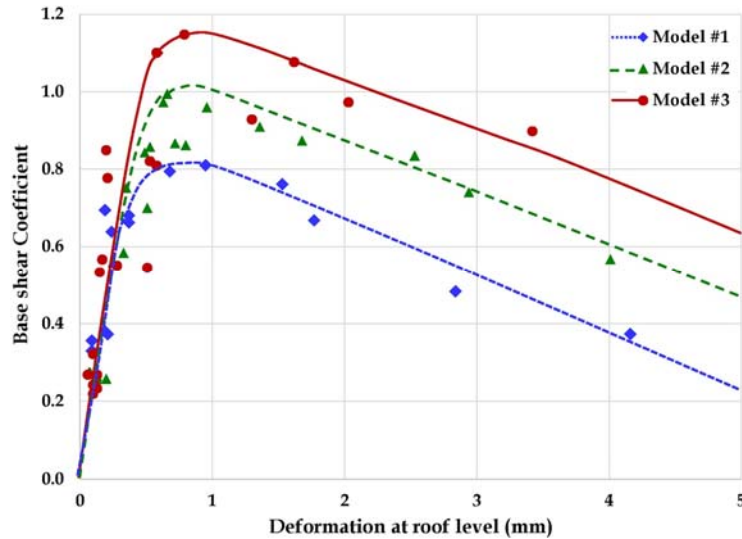Fig. 12 Diaphragm drifts variation with peak base velocity

Fig. 13 Shear resistance capacity with deformation

4.3 Force - displacement response

The shear force developed in the house models has been analyzed based on the recorded displacement and acceleration response time histories. The relationship between the shear coefficient (ratio between base shear resistance and the weight of the model) and corresponding roof level displacement is shown in Fig. 13.

Results indicate that, the shear resistance of the model 3 was larger than for the other two models. As can be seen, for the smaller deformation range, when damage observed in the models was less, a difference in lateral base shear between the models was not observed. However, after cracking, house model with better roof connection showed a higher shear resistance. The maximum base shear coefficient for models 1, 2 and 3 were 0.81, 0.99 and 1.15, respectively. These results indicate that, better roof connection had a positive effect on the shear strength of the house models.

4.4 Stiffness degradation

One of the critical parameters used in seismic design is the stiffness. Masonry structures in general do not exhibit linear behavior. However, to assess the phenomenon of stiffness degradation, stiffness (K_p) was calculated for representative cycles.

Stiffness was normalized with respect to the initial stiffness (K_o) of the corresponding house models. The degradation of stiffness in the models observed in the shaking table is summarized in Fig. 14. The decay of stiffness was observed at low ratios of drift, even before first cracking became apparent. It should be noted the value of stiffness decay were plotted after first crack. As can be shown in the Fig. 14, the value of stiffness was dropped significantly initially with a small increase in displacement. Stiffness degradation among the models 1, 2 and 3 shows significant variation indicate that roof integrity had an effect on the stiffness of the models.
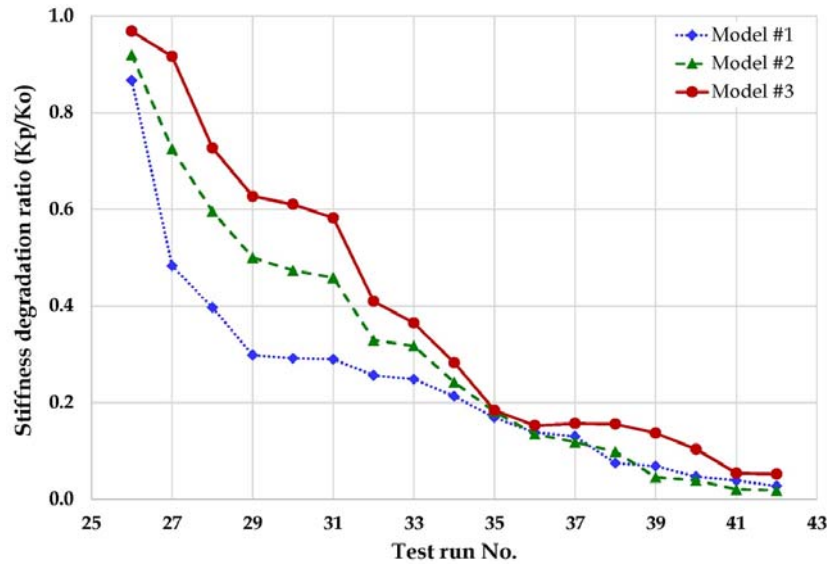
Fig. 14 Variations of stiffness of the test models

Table 4 Comparison of important seismic parameters

Strength Parameters	House model		
	1	2	3
Peak base velocity (cm/s)	8.48	8.48	12.73
In-plane drift (%)	0.48	0.35	0.32
Out-of-plane drift (%)	0.26	0.13	0.10
Shear resistance (kN)	1.83	2.25	2.60

5. Conclusions

The effect of the roof diaphragm on dynamic behavior of the masonry structures was investigated. Three types of roof diaphragm condition of masonry structure were applied; no roof, roof connected to two walls and roof connected to all four walls. The seismic performance parameters for each model were summarized in Table 4.

Based on the testing conducted during this study, the key findings were as follows:

• The roof diaphragm played an important role in failure mode of house models.

• The shear resistance value in models with proper roof connection was larger than model without a roof and model with partially connected roof.

• The evaluation of results reveals the model with proper roof diaphragm connection; as the lateral stiffness, maximum strength, yield displacement and ductility in the building are larger than model without a roof and model with partially connected roof.

The test result clearly shows that, models with roof diaphragm to wall global response of the structure, preventing the occurrence of local out-of-plane damage mechanisms which occur in the model without a roof. So, the model with proper roof diaphragm connection was able to withstand stronger shaking than the model without a roof diaphragm connection.

Acknowledgements

Reference

ASTM (American Society for Testing Materials) E 519-10. (2010), *Standard test method for diagonal tension (shear) in masonry assemblages*, Annual Book of ASTM Standards, ASTM International, West Conshohocken PA.

Araújo, A.S., Oliveira, D.V. and Lourenço, P.B. (2014), "Numerical study on the performance of improved masonry-to-timber connections in traditional masonry buildings", *Eng. Struct.*, **80**, 501-513.

Benjamin, J.R. (1988), *A criterion for determining exceedance of the operating basis earthquake*, Report No. EPRI NP-5930, Electrical Power Research Institute, Palo Alto, California, USA.

British Standards Institution (1999), BS EN 1052-1:1999, Methods of test for masonry - Part 1: Determination of compressive strength, BSI, London, UK.

British Standards Institution (2002), BS EN 1052-3:2002, Methods of test for masonry - part 3: determination of initial shear strength, BSI, London, UK.

International Conference of Building Officials (ICBO) (1997), Uniform Building Code, ICBO, Whittier, CA, USA.

Lourenço, P.B., Mendes, N., Ramos, L.F. and Oliveira, D.V. (2011), "Analysis of masonry structures without box behavior", *Int. J. Architec. Herit.: Conserv., Anal. Rest.*, **5**(4-5), 369-382.

Magenes, G., Penna, A., Senaldi, I.E., Galasco, A. and Rota, M. (2013), "Experimental investigation on the effect of diaphragm in-plane stiffness on the seismic response of masonry buildings", *12ᵗʰ Canadian Masonry Symposium*, Vancouver B.C., Canada.

Magenes. G., Penna, A., Senaldi, I.E., Rota, M. and Galasco, A. (2014), "Shaking table test of a strengthened full scale stone masonry building with flexible diaphragms", *Int. J. Architec. Herit.*, **8**(3), 349-375.

Rota, M., Penna, A., Strobbia, C. and Magenes, G. (2011), "Typological seismic risk maps for Italy", *Earthq. Spectra*, **27**(3), 907-926.

Sathiparan, N., Mayorca, P., Nesheli, N., Ramesh, G. and Meguro, K. (2005), "In-Plane and Out-of-Plane behavior of PP-band retrofitted masonry wallettes",*4ᵗʰ International Symposium on New Technologies for Urban Safety of Mega Cities in Asia*, Nanyang Technological University, Singapore.

Sathiparan, N., Mayorca, P. and Meguro, K. (2012), "Shaking table test on one-quarter scale models of masonry houses retrofitted with PP-band mesh", *Earthq. Spectra*, **28**(1), 277-299.

Sathiparan, N. and Meguro, K. (2012), "Seismic behavior of low earthquake-resistant arch-shaped roof masonry houses retrofitted by PP-band meshes", *Practice Period. Struct. Des. Constr.*, **17**(2), 54-64.

Senaldi, I., Magenes, G., Penna, A., Galasco, A. and Rota, M. (2013), "The effect of stiffened floor and roof diaphragms on the experimental seismic response of a full scale unreinforced stone masonry building", *J. Earthq. Eng.*, **18**(3), 407-443.

Simsir C.C., Aschheim, M.A. and Abrams, D.P. (2004), "Out-of-plane dynamic response of unreinforced masonry bearing walls attached to flexible diaphragms", *13ᵗʰ World Conference on Earthquake Engineering*, Vancouver B.C., Canada.

Tomaževič, M., Velechovsky, T. and Weiss, P. (1992), "The effect of interventions in the floor structural system on the seismic resistance of historic stone-masonry buildings: An experimental study", *10ᵗʰ World*

Conference on Earthquake Engineering, Madrid, Spain.

KT